

Flame acceleration and transition to detonation in a channel with triangular obstacles

Huahua Xiao¹, Elaine S. Oran²

¹State Key Laboratory of Fire Science, University of Science and Technology of China, Hefei, Anhui province 230027, P. R. China

²University of Maryland, College Park, Maryland 20742, USA

1 Introduction

Flame acceleration and deflagration-to-detonation transition (DDT) are of great importance in the research areas of explosion safety [1-4] and propulsion applications [5, 6]. DDT is a very complex process involving flow/combustion instabilities, turbulence, boundary layer effects, shock-flame and shock-shock interactions, and detonation initiation. The spatial scales in DDT processes can cover up to 12 orders of magnitude in real systems. This is one of the major factors making the problem computationally challenging [3]. In recent years, significant insights into DDT phenomena have been gained in scenarios with [7-12] and without obstructions [3, 13, 14]. Nonetheless, because DDT is a rapid, nonlinear and complex process, first-principle understanding and quantitative modeling of DDT still remain a major challenge.

Tubes or channels equipped with obstacles are generally used to investigate DDT in experiments and numerical simulations [4, 8, 11, 12] since obstacles can cause significant hydrodynamic disturbances to the flow and thus promote faster flame acceleration and sooner detonation initiation than smooth channels. In such systems, the mechanisms underlying flame acceleration include thermal expansion of hot combustion products, flame-vortex interactions, and Rayleigh-Taylor, Richtmyer-Meshkov and Kelvin-Helmholtz instabilities arising from effects of pressure waves and shear flows. These physical phenomena lead to a corrugated flame or even a turbulent flame, which further facilitates the acceleration of flame and flow. The quickly accelerating flow produces strong shocks and creates conditions in which DDT can occur. Detonations can be initiated in the vicinity of corrugated or turbulent flames through Zeldovich reactivity-gradient mechanism as hot spots are created by Mach-stem reflections from obstacles [10-12]. Sometimes, focusing of shock waves with sufficient strength can deposit enough energy in a small spot and initiate a detonation directly [7, 8, 15]. Other possible explanations of DDT include hydraulic resistance [16] and thermal runaway of fast flames [17]. Majority of previous studies were conducted using rectangular or cylindrical obstacles [3, 4]. Few studies were on scenarios with triangular obstacles on walls, although this type of geometry can represent surface roughness.

This work presents numerical simulations of flame acceleration and DDT in a highly reactive hydrogen-oxygen mixture in a channel with triangular obstacles. The unsteady fully compressible Navier-Stokes (NS) equations are solved using high-order schemes and adaptive mesh refinement (AMR). The influence of blockage ratio on DDT is also examined.

2 Physical and numerical Models

The governing equations solved in the calculations are the two-dimensional fully compressible reactive NS equations coupled to a chemical model of stoichiometric hydrogen-oxygen mixture. Details of the equations can be found elsewhere [8, 18]. A chemical-diffusive model [11, 19], which takes into account both transport properties and chemical reaction rate, is adopted to calculate the chemical heat release and conversion of reactants to products of the mixture at 298 K and 1 atm. The reaction rate is modeled using a single-step Arrhenius-type kinetics $\dot{\omega} = A\rho Y \exp(E_a/RT)$, where T , Y , ρ , A , E_a and R are the temperature, unburned mass fraction, density, pre-exponential factor, activation energy, and universal gas constant, respectively. This type of model can appropriately take into account the dependency of flame speed on pressure [9].

A Godunov algorithm, which is third-order accurate in space and second-order in time [20], is used to solve the governing equations. Block-structured AMR based on the BoxLib library [21] allows the computations to resolve the important flow structures such as boundary layer, flame, and pressure waves. Figure 1 is a schematic diagram of the computational domain. The configuration is a 2 cm high and 30 cm long channel with uniform triangular obstacles placed continuously along the upper and bottom walls. The obstacles are modeled by an immersed boundary method [22]. The obstacle width is 5.8 mm. The obstacle height h is defined using the blockage ratio br , i.e., $h = w \cdot br$, where $w = 2$ cm is the channel height. Four blockage ratios, $br = 0.1, 0.3, 0.5$, and 0.7 , are chosen in the calculations, corresponding to obstacle heights $h = 0.1, 0.3, 0.5$, and 0.7 cm, respectively.

The smallest grid size is $15.6 \mu\text{m}$, corresponding to 16 computational cells per laminar flame thickness under the initial conditions. Grid resolution tests showed that the cell size is adequate for simulating the DDT process in this work. The ignition zone is a circular region of hot, burned gas with a radius of 1 mm. The center of the initial flame is located on the axis 5.8 mm from the left end wall.



Figure 1. Computational domain of a channel with triangular obstacles. Adiabatic, reflecting and no-slip boundary conditions are applied for the walls and obstacle surfaces. Four obstacle heights $h = 1, 3, 5$, and 7 mm are used, corresponding to blockage ratio $br = 0.1, 0.3, 0.5$, and 0.7 , respectively. Initial flame radius is 1 mm.

3 Numerical results

Figure 2 show selected temperature and schlieren fields of flame acceleration and DDT in the channel at a blockage ratio of 0.3. After ignition, the flame expands circularly outward, as shown at 0.052 ms. Under

confinement, the flame initially accelerates due to thermal expansion of combustion products, as discussed in [18]. Vortices are generated between triangles as the accelerating flow passes over the obstacles, as shown by the schlieren field at 0.133 ms. The flame is stretched and convoluted when it approaches the obstacles and interacts with the vortices. The lateral edges of the flame front become fragmented as the flame continues to accelerate. The flame corrugation further accelerates the flow and produces compression waves ahead of the flame front, as shown by the schlieren at 0.171 ms. Detonations, D1 and D2, are initiated near obstacles at upper and bottom walls, respectively, as shown at 0.221 ms. These two detonations sweep through the shocked region moving towards the channel center (see 0.223 ms). Finally they join together and propagate into the unburned gas, as shown at 0.239 ms.

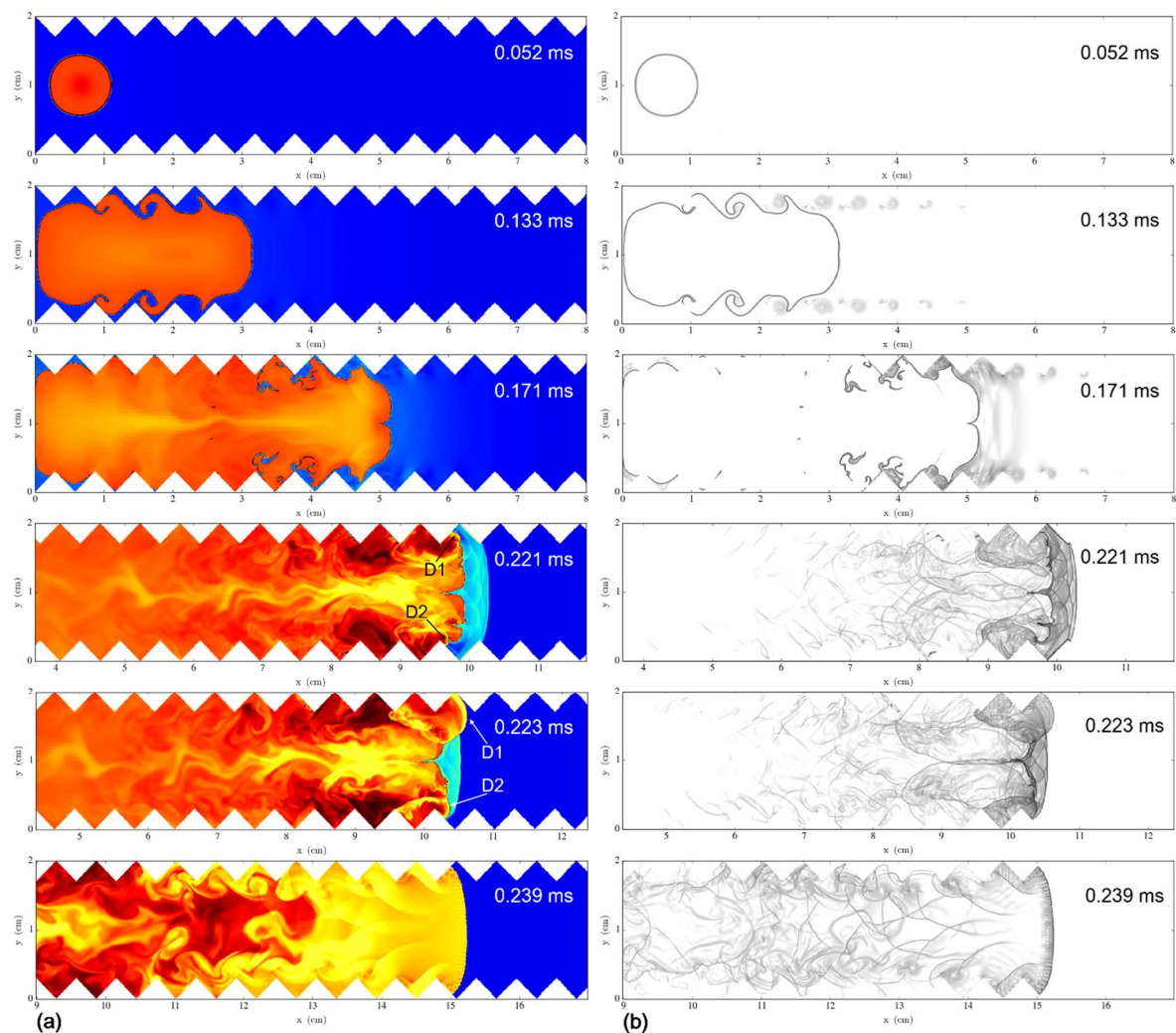


Figure 2. Sequences of (a) temperature and (b) schlieren fields of flame acceleration and transition to detonation in a stoichiometric hydrogen-oxygen mixture in a channel with triangular obstacles at a blockage ratio 0.3. D1 and D2 denote detonations.

Figure 3 presents the speed of the leading edge of reaction front as a function of position. The flame acceleration rate increases with increasing the blockage ratio. The flame acceleration is significantly smaller

at the low blockage ratio $br = 0.1$ than the other cases, and thus the distance required for DDT to occur is much larger. For the case with high blockage ratio $br = 0.7$, DDT does not occur although the flame acceleration rate is large. Instead, the flame propagates at speed of about 1400 m/s that is approximately 1/2 of the CJ detonation speed 2840 m/s. This is typical of choking regime of flame propagation [23]. In the choking regime, the complex of flame and shock propagates supersonically.

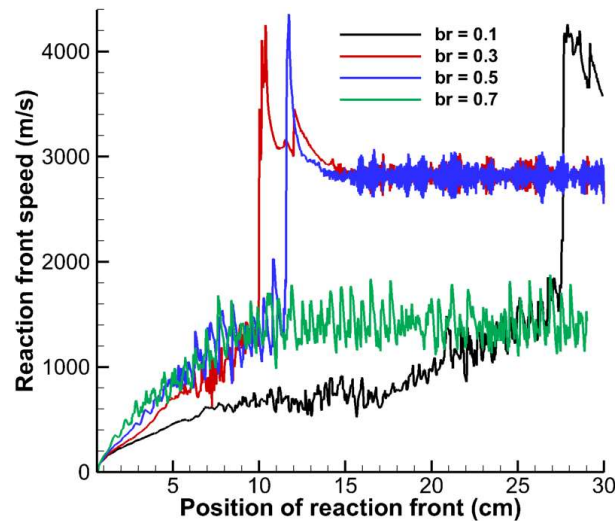


Figure 3. Speed of leading reaction front as a function of position for blockage ratios $br = 0.1, 0.3, 0.5,$ and 0.7 .

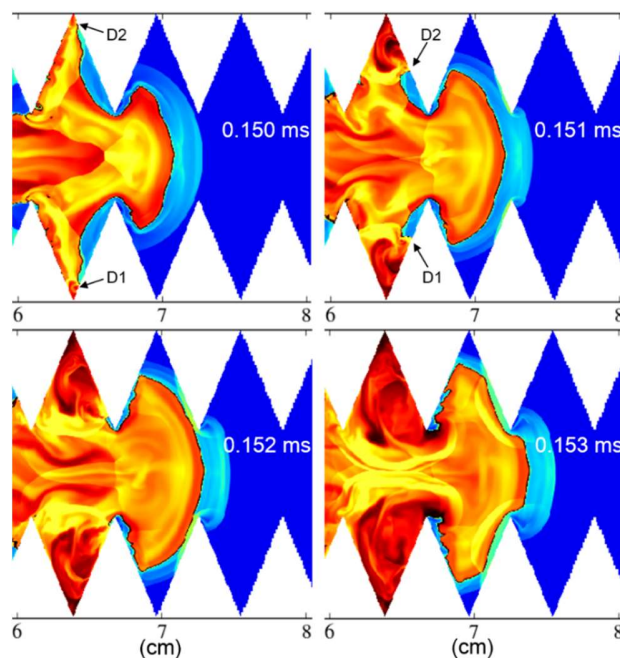


Figure 4. Detonation initiation and failure at corners between neighboring triangles in the case with a blockage ratio of 0.7. D1, D2–detonations.

Although a full DDT does not develop at $br = 0.7$, detonation initiation and failure repeatedly occur during the choking flame propagation. Figure 4 shows detonation initiation and failure at the corners between neighboring obstacles for blockage ratio $br = 0.7$. As the shock-flame complex passes over a pair of opposite obstacles, the lateral flame front propagates into the corner of two neighboring triangles at both the upper and bottom walls. When the flame and shock interact in the vicinity of the corner vertex, a detonation is triggered, as shown as 0.15 ms. The detonation travels in the narrow unburned gap along the left surface of the obstacle adjacently ahead, as shown at 0.151 and 0.152 ms. However, the detonation fails when it reaches the vertex of the obstacle because the unburned gas space becomes too narrow for the detonation to survive, as shown at 0.153 ms. This detonation initiation and failure process repeats every time the shock-flame complex passes over a pair of opposite obstacles until the end of combustion.

The result shown above is only part of the work that has been conducted to explore flame acceleration and DDT in a channel with triangular obstacles. More results will be described and discussed in the presentation.

Acknowledgments

This study was supported by University of Science and Technology of China through the 1000-Talent Program for Young Outstanding Scientists. The authors thank Dr. Ryan Houim for his significant contribution to the development of the numerical method.

References

- [1] Oran E.S. (2015). From catastrophic accidents to the creation of the universe. *P Combust Inst.* 35: 1.
- [2] Middha P., Hansen O.R. (2008). Predicting deflagration to detonation transition in hydrogen explosions. *Process Safety Progress.* 27: 192.
- [3] Oran E.S., Gamezo V.N. (2007). Origins of the deflagration-to-detonation transition in gas-phase combustion. *Combust Flame.* 148: 4.
- [4] Ciccarelli G., Dorofeev S. (2008). Flame acceleration and transition to detonation in ducts. *Progress in Energy and Combustion Science.* 34: 499.
- [5] Huang Y., Tang H., Li J., Wang J. (2011). Deflagration-to-detonation transition of kerosene-air mixtures in a small-scale pulse detonation engine. *Proceedings of the Institution of Mechanical Engineers Part G- Journal of Aerospace Engineering.* 225: 441.
- [6] Roy G.D., Frolov S.M., Borisov A.A., Netzer D.W. (2004). Pulse detonation propulsion: challenges, current status, and future perspective. *Progress in Energy and Combustion Science.* 30: 545.
- [7] Goodwin G.B., Houim R.W., Oran E.S. (2017). Shock transition to detonation in channels with obstacles. *P Combust Inst.* 36: 2717.
- [8] Goodwin G.B., Houim R.W., Oran E.S. (2016). Effect of decreasing blockage ratio on DDT in small channels with obstacles. *Combust Flame.* 173: 16.
- [9] Ogawa T., Gamezo V.N., Oran E.S. (2013). Flame acceleration and transition to detonation in an array of square obstacles. *Journal of Loss Prevention in the Process Industries.* 26: 355.
- [10] Kessler D.A., Gamezo V.N., Oran E.S. (2010). Simulations of flame acceleration and deflagration-to-detonation transitions in methane-air systems. *Combust Flame.* 157: 2063.

- [11] Gamezo V.N., Ogawa T., Oran E.S. (2008). Flame acceleration and DDT in channels with obstacles: Effect of obstacle spacing. *Combust Flame*. 155: 302.
- [12] Gamezo V.N., Ogawa T., Oran E.S. (2007). Numerical simulations of flame propagation and DDT in obstructed channels filled with hydrogen-air mixture. *P Combust Inst*. 31: 2463.
- [13] Houim R.W., Ozgen A., Oran E.S. (2016). The role of spontaneous waves in the deflagration-to-detonation transition in submillimetre channels. *Combustion Theory and Modelling*. 20: 1068.
- [14] Kuznetsov M., Alekseev V., Matsukov I., Dorofeev S. (2005). DDT in a smooth tube filled with a hydrogen-oxygen mixture. *Shock Waves*. 14: 205.
- [15] Maeda S., Minami S., Okamoto D., Obara T. (2016). Visualization of deflagration-to-detonation transitions in a channel with repeated obstacles using a hydrogen-oxygen mixture. *Shock Waves*. 26: 573.
- [16] Brailovsky I., Sivashinsky G.I. (2000). Hydraulic resistance as a mechanism for deflagration-to-detonation transition. *Combust Flame*. 122: 492.
- [17] Kagan L., Sivashinsky G. (2017). Parametric transition from deflagration to detonation: Runaway of fast flames. *P Combust Inst*. 36: 2709.
- [18] Xiao H., Houim R.W., Oran E.S. (2015). Formation and evolution of distorted tulip flames. *Combust Flame*. 162: 4084.
- [19] Kaplan C.R., Ozgen A., Oran E.S. (2018). Chemical-diffusive models for flame acceleration and transition-to-detonation: genetic algorithm and optimisation procedure. *Combust Theor Model*. In press: <https://doi.org/10.1080/13647830.2018.1481228>.
- [20] Houim R.W., Kuo K.K. (2011). A low-dissipation and time-accurate method for compressible multi-component flow with variable specific heat ratios. *Journal of Computational Physics*. 230: 8527.
- [21] Boxlib, Center for Computational Sciences and Engineering, University of California, Berkeley. 2015.
- [22] Chaudhuri A., Hadjadj A., Chinnayya A. (2011). On the use of immersed boundary methods for shock/obstacle interactions. *Journal of Computational Physics*. 230: 1731.
- [23] Lee J.H., Knystautas R., Chan C.K. (1985). Turbulent flame propagation in obstacle-filled tubes. *P Combust Inst*. 20: 1663.